

Grzegorz SIKORA\*, Andrzej MISZCZAK\*

## THE CHANGE OF FRICTION AND LOAD-CARRYING CAPACITY OF THE JOURNAL BEARING WITH THE CONSIDERATION OF THE OIL AGEING

### ZMIANY SIŁY NOŚNEJ I SIŁY TARCIA W POPRZECZNYM ŁOŻYSKU ŚLIZGOWYM PRZY UWZGLĘDNIENIU STARZENIA SIĘ OLEJU

#### Key words:

oil ageing, slider bearing, viscosity changes in exploitation time, numerical calculations, friction force, carrying capacity, friction coefficient

#### Słowa kluczowe:

starzenie oleju, łożysko ślizgowe, zmiany lepkości od czasu eksploatacji, obliczenia numeryczne, siła tarcia, siła nośna, współczynnik tarcia

#### Abstract

This paper presents numerical calculations of the hydrodynamic pressure distribution, carrying capacity, and friction coefficient in the gap of a journal bearing. The analysed bearing is lubricated using motor oil. In this paper, oil ageing and temperature influence on viscosity are taken into account. Viscosity changes in the pressure and shear rate are not considered. These changes will be considered in other papers.

---

\* Gdynia Maritime University, ul. Morska 81-87, 81-225 Gdynia, Poland,  
e-mails: g.sikora@wm.am.gdynia.pl, miszczak@wm.am.gdynia.pl, phone: + 48 58 5586438.

For the hydrodynamic lubrication analysis, laminar flow of the lubrication fluid and non-isothermal lubrication model of the journal bearing were assumed. As the constitutive equation, the classical, Newtonian model was used. This model was extended by the viscosity changes in temperature and exploitation time. For the considerations, the cylindrical journal bearing with the finite length and smooth bearing, with the full angle of wrap were taken.

## INTRODUCTION

During exploitation time, lubrication oil is subjected to the ageing process. Verification of the oil condition is based on oil analysis in laboratory or with the sensors of oil condition [L. 1, 2]. Oil condition is being compared to the new oil parameters and referred to the limit state, which should be not exceeded. Reaching of the limit state even only by the one parameter causes that the oil does not fulfil its basic function [L. 3]. In this case, proper actions have to be undertaken, e.g. purifying, refilling (marine engines), and oil change.

The above-described issues are well known and explored. Problem occurs if there is a need to take into account the changes in the oil due to ageing, exploitation, and flow parameters at the friction node design stage. This problem is a subject of the author's research.

In the thin layer of oil film, the constancy of density and heat transfer coefficient from the temperature were assumed [L. 4–7]. Viscosity changes in exploitation time were modelled as an exponential function based on the experimental research.

For the experimental research, the lubrication oil Castrol EDGE 5W30 was taken. This oil was exploited in the 1.8l petrol engines of the personal car Honda FRV. Oil samples were taken in the first stage of exploitation approximately every 300km and then approximately every 3000 km. The sample is the clean oil and the last one is a sample after 16 235 km.

Viscosity changes were measured on the Haake Mars 3 rheometer in the laboratory of Gdynia Maritime University. Viscosity changes as a function of temperature, shear rate, and exploitation time were measured.

Results of the experimental research, as the function exploitation time, for the temperature of 90°C and constant shear rate, are shown in **Fig. 1**. Viscosity changes in temperature are shown in **Fig. 2**. In the literature, exploitation time is given in the working hours, motion hours, or millage. By the exploitation time that corresponds to the millage of 12 000 km, a lowering of the dynamic viscosity occurs. This lowering might be caused by measurement error or by the temporary lowering of the viscosity due to a petrol leak into the engine oil, before the sample was taken.

The curves of the viscosity changes, which are shown on the **Fig. 2**, have been described as exponential equations. These equations and each coefficient are shown in **Tab 1**.

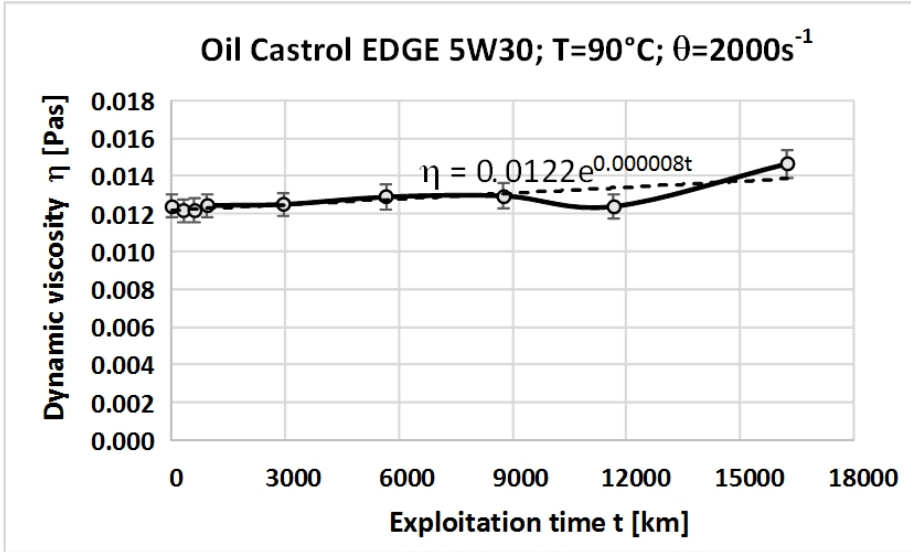


Fig. 1. Dynamic Viscosity changes of the motor oil Castrol EDGE 5W30 in exploitation time

Rys. 1. Zmiany lepkości dynamicznej oleju silnikowego Castrol EDGE 5W30 od czasu eksploatacji

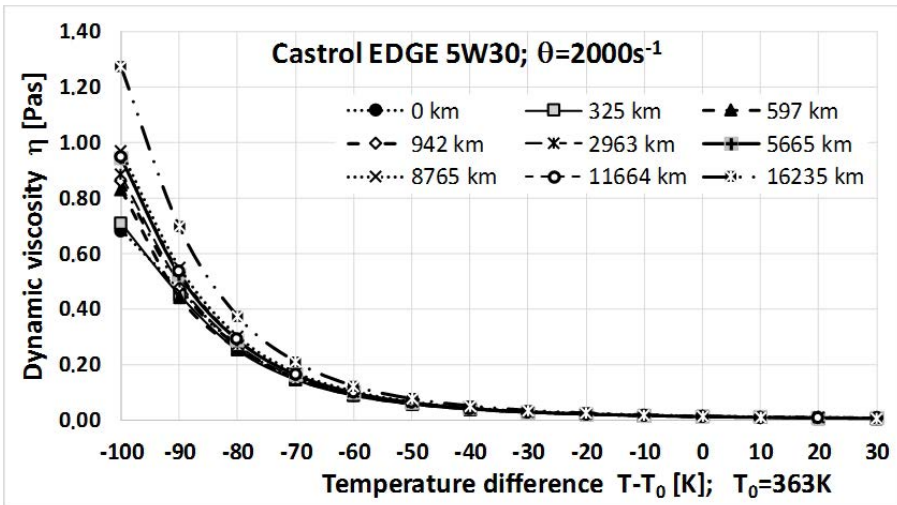


Fig. 2. Dynamic viscosity changes in temperature for the motor oil Castrol EDGE 5W30 in different exploitation times

Rys. 2. Zmiany lepkości dynamicznej od temperatury dla oleju silnikowego Castrol EDGE 5W30 przy różnych czasach eksploatacji

**Table 1. Equations of the changes of the dynamic viscosity in temperature T-T<sub>0</sub> for the different exploitation times of the Castrol EDGE 5W30 motor oil**

Tabela 1. Równania zmian lepkości dynamicznej od temperatury T-T<sub>0</sub> dla różnych czasów eksploatacji oleju Castrol EDGE 5W30

Exploitation time [km]	Trend line equation $\eta = \eta_0 e^{-\delta(T-T_0)}$	Coefficient $\delta$ [1/K]	Characteristic dimensional viscosity $\eta_0$ [Pas]
0	$\eta = 0.01296e^{0.036049(T-T_0)}$	0.036049	0.01296
325	$\eta = 0.01264e^{0.036044(T-T_0)}$	0.036044	0.01264
597	$\eta = 0.01263e^{0.03646(T-T_0)}$	0.036460	0.01263
942	$\eta = 0.01296e^{0.036049(T-T_0)}$	0.036762	0.01286
2963	$\eta = 0.01296e^{0.036049(T-T_0)}$	0.037018	0.01296
5665	$\eta = 0.01296e^{0.036049(T-T_0)}$	0.037281	0.01338
8765	$\eta = 0.01296e^{0.036049(T-T_0)}$	0.037675	0.01351
11664	$\eta = 0.01296e^{0.036049(T-T_0)}$	0.037843	0.01287
16235	$\eta = 0.01296e^{0.036049(T-T_0)}$	0.039739	0.01447

## BASIC EQUATIONS

Analysis of the hydrodynamic lubrication of the journal bearings by the laminar and non-isothermal flow includes solving of the momentum conservation equation, fluid flow equation, and energy conservation equation in the following forms [L. 4–11]:

$$\rho \frac{dv}{dt} = \text{Div } \mathbf{S}, \quad (1)$$

$$\text{div}(\rho \mathbf{v}) = 0, \quad (2)$$

$$\text{div}(\kappa \text{grad } T) + \text{div}(\mathbf{v}\mathbf{S}) - \mathbf{v}\text{Div}\mathbf{S} = \rho \frac{d(c_v T)}{dt}, \quad (3)$$

where:

- $c_v$  – specific heat of the oil by the constant volume [J/(kgK)],
- $t$  – time [s],
- $\mathbf{v}$  – velocity vector of the oil [ $\text{m}\cdot\text{s}^{-1}$ ],
- $\mathbf{S}$  – stress tensor of the oil with the coordinates  $\tau_{ij}$  for  $i,j = \phi, r, z$  [Pa],
- $T$  – oil temperature distribution in the lubrication gap [K],
- $\rho$  – oil density [ $\text{kg}\cdot\text{m}^{-3}$ ],
- $\kappa$  – heat transfer coefficient of the lubrication oil [W/(mK)].

Constitutive relations, which describe relations between stress tensor coefficients and velocity strain tensor of the oil, can be presented in the following form [L. 5, 6, 8, 9]:

$$S = -p \mathbf{I} + \eta_a(p, T, \theta, t) \mathbf{A}_1. \quad (4)$$

Velocity strain tensor is described by the following relation [L. 5, 6]:

$$\mathbf{A}_1 \equiv \mathbf{L} + \mathbf{L}^T, \quad \mathbf{L} \equiv \text{grad } \mathbf{v}, \quad (5)$$

where:

- $\mathbf{A}_1$  – first velocity strain tensor with the coordinates  $\Theta_{ij}$  [ $s^{-1}$ ],
- $\mathbf{I}$  – unity tensor,
- $\mathbf{L}$  – velocity gradient tensor [ $s^{-1}$ ],
- $p$  – hydrodynamic pressure [Pa],
- $\eta_a$  – apparent viscosity coefficient [Pa·s],
- $\theta$  – shear rate [1/s].

For further calculations, the dynamic viscosity was assumed as the function dependent on the temperature [L. 5, 6] and exploitation time  $\eta_a = \eta_a(T, t)$  [L. 8, 11]. The function of the dynamic viscosity is presented as the product of the dimensional value and dimensionless relations, which take each influence into account as follows:

$$\eta_a = \eta_o \cdot \eta_{1a}; \quad \eta_{1a} = \eta_{1T} \cdot \eta_{1t},$$

$$\eta_{1T}(\phi, z, r) \equiv B \cdot e^{-\delta_T(T-T_o)} = B \cdot e^{-Q_{Br}T_1}, \quad \eta_{1t}(t) \equiv D \cdot e^{\delta_i t} = D \cdot e^{\delta_{1t} t}, \quad (6)$$

where:

- $\eta_{1a}$  – total dimensionless dynamic viscosity,
- $\eta_o$  – characteristic dimensional value of the dynamic viscosity by the very small shear rate and characteristic temperature  $T_o$  and pressure  $p_o$ ,
- $\eta_{1T}$  – dimensionless dynamic viscosity, dependent on temperature,
- $\eta_{1t}$  – dimensionless dynamic viscosity, dependent on exploitation time,
- $\delta_i, \delta_{1t}$  – dimensional and dimensionless material coefficient, including viscosity changes in time,
- $\delta_T$  – material coefficient, including viscosity changes in temperature [1/K],
- $\kappa_o$  – dimensional heat transfer coefficient of the oil [W/(mK)],
- $\omega$  – angular velocity of the journal [1/s],
- $Q_{Br} = R^2 \omega^2 \eta_o \delta_T / \kappa_o$  – dimensionless coefficient of the viscosity changes in temperature,
- $\chi$  – positive coefficient, interpreted as a time constant [s],

- B,D – dimensionless coefficients which include different values of the dimensional characteristic  $\eta_0$ , which is designated from the measurements on the rheometer, by the different influences (temperature, exploitation time, pressure, shear rate),
- R – journal radius [m],
- $T_1$  – dimensionless temperature,
- $T_0$  – dimensional characteristic value of the temperature [K],
- $t_1$  – dimensionless time.

Equations of momentum, fluid flow, and energy conservation have been transformed into dimensionless forms and estimated. Parts in the height of the radial clearance have been neglected. Using of the small parameter method, the system of equations has been spread into two subsystems. The first one took flow parameters changes in exploitation time into account. The second one took changes of those parameters on dynamic viscosity of the oil into account [L. 5, 6].

After double integration of the first and third momentum equation and after that substituting of the boundary conditions, the first and the third dimensionless component of the velocity vector have been obtained [L. 5, 6]. By the transforming of the fluid flow equation and substituting into it the first and the third component of the velocity vector, integration and substituting of the boundary conditions of this form, the second component of the velocity vector was obtained [L. 5, 6]. Substituting in the same solution the second set of the boundary conditions, the Reynolds-type equation was obtained [L. 5, 6]. This equation received the following form:

$$\frac{\partial}{\partial \phi} \left( \frac{h_{p1}^3}{\eta_{1t}(t)} \frac{\partial p_1^{(0)}}{\partial \phi} \right) + \frac{1}{L_1^2} \frac{\partial}{\partial z_1} \left( \frac{h_{p1}^3}{\eta_{1t}(t)} \frac{\partial p_1^{(0)}}{\partial z_1} \right) = 6 \frac{\partial h_{p1}}{\partial \phi}, \quad (7)$$

where:

- $h_{p1}$  – dimensionless height of the lubrication gap, which depends on the related eccentricity  $\lambda$  and parallelism of the journal axis and bushing axis  $\gamma$  [L. 5],
- $L_1$  – dimensionless length of the bearing,
- $p_1$  – dimensionless pressure,
- $z_1$  – dimensionless axial coordinate of the cylindrical system,
- $\phi$  – peripheral coordinate of the cylindrical system,
- $\eta_{1t}(t)$  – dimensionless dynamic viscosity, which depends on the exploitation time.

Hydrodynamic pressure distribution was obtained from the Reynolds-type equation. This equation has been developed from the basics from the motion equations using classical relations used for the thin boundary layer.

Proceeding similarly with the second equation system, the Reynolds-type equation was obtained, with which the hydrodynamic pressure distribution can be obtained [L. 5, 6]:

$$\begin{aligned} & \frac{\partial}{\partial \phi} \left[ \frac{h_{p1}^3}{\eta_{lt}} \left( \frac{\partial p_{10}^{(1)}}{\partial \phi} \right) \right] + \frac{1}{L_1^2} \frac{\partial}{\partial z_1} \left[ \frac{h_{p1}^3}{\eta_{lt}} \left( \frac{\partial p_{10}^{(1)}}{\partial z_1} \right) \right] = \\ & = 12 \left\{ \frac{\partial}{\partial \phi} \left[ \left( \int_0^{h_{p1}} \left( \int_0^{r_1} T_1^{(0)} \frac{\partial v_1^{(0)}}{\partial r_1} dr_1 \right) dr_1 - \int_0^{h_{p1}} \frac{r_1}{h_{c1}} \left( \int_0^{h_{p1}} T_1^{(0)} \frac{\partial v_1^{(0)}}{\partial r_1} dr_1 \right) dr_1 \right) \right] + \right. \\ & \left. + \frac{1}{L_1^2} \frac{\partial}{\partial z_1} \left[ \left( \int_0^{h_{p1}} \left( \int_0^{r_1} T_1^{(0)} \frac{\partial v_3^{(0)}}{\partial r_1} dr_1 \right) dr_1 - \int_0^{h_{p1}} \frac{r_1}{h_{c1}} \left( \int_0^{h_{p1}} T_1^{(0)} \frac{\partial v_3^{(0)}}{\partial r_1} dr_1 \right) dr_1 \right) \right] \right\}, \end{aligned} \tag{8}$$

Dimensionless carrying capacity  $C_1^{(0)}$  and dimensionless correction of the carrying capacity  $C_{10}^{(0)}$  have been obtained from the following relations [L. 5, 6]:

$$C_1^{(0)} = \sqrt{\left( \int_{-1}^{+1} \left( \int_0^{\phi_k} p_1^{(0)} \cos \gamma \sin \phi \, d\phi \right) dz_1 \right)^2 + \left( \int_{-1}^{+1} \left( \int_0^{\phi_k} p_1^{(0)} \cos \gamma \cos \phi \, d\phi \right) dz_1 \right)^2}, \tag{9}$$

$$C_{10}^{(0)} = \sqrt{\left( \int_{-1}^{+1} \left( \int_0^{\phi_k} p_{10}^{(0)} \cos \gamma \sin \phi \, d\phi \right) dz_1 \right)^2 + \left( \int_{-1}^{+1} \left( \int_0^{\phi_k} p_{10}^{(0)} \cos \gamma \cos \phi \, d\phi \right) dz_1 \right)^2}. \tag{10}$$

Dimensionless friction  $F_{r1}^{(0)}$  and dimensionless correction of the friction  $F_{r10}^{(0)}$  have been obtained from the following relations [L. 5, 6]:

$$\begin{aligned} F_{r1}^{(0)} &= \int_{-1}^{+1} \left[ \int_0^{\phi} \left( \eta_{lt} \frac{\partial v_1^{(0)}}{\partial r_1} \right)_{r_1=h_{p1}} d\phi \right] dz_1 = \\ &= \int_{-1}^{+1} \left[ \int_0^{2\pi} \left( \eta_{lt} \frac{\partial v_{1s}^{(0)}}{\partial r_1} \right)_{r_1=h_{p1}} d\phi \right] dz_1 + \int_{-1}^{+1} \left[ \int_0^{\phi_k} \left( \eta_{lt} \frac{\partial v_{1p}^{(0)}}{\partial r_1} \right)_{r_1=h_{p1}} d\phi \right] dz_1, \end{aligned} \tag{11}$$

$$Fr_{10}^{(1)} = \int_{-1}^{+1} \left[ \int_0^{\phi} \left( \eta_{1r} \frac{\partial v_{10}^{(1)}}{\partial r_1} \right)_{r_1=h_{p1}} d\phi \right] dz_1 =$$

$$\int_{-1}^{+1} \left[ \int_0^{2\pi} \left( \eta_{1r} \frac{\partial v_{10s}^{(1)}}{\partial r_1} \right)_{r_1=h_{p1}} d\phi \right] dz_1 + \int_{-1}^{+1} \left[ \int_0^{\phi_k} \left( \eta_{1r} \frac{\partial v_{10p}^{(1)}}{\partial r_1} \right)_{r_1=h_{p1}} d\phi \right] dz_1, \tag{12}$$

Dimensionless friction coefficient  $\left(\frac{\mu}{\psi}\right)_1^{(0)}$  and dimensionless correction of the friction coefficient  $\left(\frac{\mu}{\psi}\right)_{10}^{(0)}$  have been obtained from the following relations [L. 5, 6]:

$$\left(\frac{\mu}{\psi}\right)_1^{(0)} = \frac{Fr_1^{(0)}}{C_1^{(0)}}, \tag{13}$$

$$\left(\frac{\mu}{\psi}\right)_{10}^{(1)} = \frac{Fr_{10}^{(1)}C_1^{(0)} - Fr_1^{(0)}C_{10}^{(1)}}{\left(C_1^{(0)}\right)^2}, \tag{14}$$

Total dimensional carrying capacity, friction, and the total friction coefficient are obtained from the following relations [L. 5, 6]:

$$p_1 = p_1^{(0)} + Q_{Br}p_{10}^{(1)}, \tag{15}$$

$$C_{\Sigma} = C_{1\Sigma} \cdot bR\eta_o\omega/\psi^2 = \left(C_1^{(0)} + Q_{Br}C_{10}^{(1)}\right) \cdot bR\eta_o\omega/\psi^2, \tag{16}$$

$$Fr_{\Sigma} = Fr_1 \cdot bR\eta_o\omega/\psi = \left(Fr_1^{(0)} + Q_{Br}Fr_{10}^{(1)}\right) \cdot bR\eta_o\omega/\psi, \tag{17}$$

$$\left(\frac{\mu}{\psi}\right)_{\Sigma} = \frac{Fr_{\Sigma}}{\psi C_{\Sigma}} = \left(\frac{\mu}{\psi}\right)_1^{(0)} + Q_{Br} \left(\frac{\mu}{\psi}\right)_{10}^{(1)}. \tag{18}$$

### NUMERICAL CALCULATIONS

Numerical calculations were performed using Mathcad 15 software using a finite difference method and the author’s own procedures. Dimensionless hydrodynamic pressure and dimensionless corrections of the hydrodynamic pressure were obtained from equations (7) and (8).

Carrying capacity, friction, and the friction coefficient were obtained from equations (9)-(14).



Numerical calculations were performed for the following data: dimensionless length of the bearing  $L_1 = 1$ , related eccentricity  $\lambda = 0.8$ , and the equation of the viscosity changes in time  $\eta_{lt} = e^{0.000008t}$ . Parameters of the function that describes viscosity changes in time for the different exploitation intervals were assumed from **Tab. 1**. Results of the numerical calculations of carrying capacity, friction, and the friction coefficient are shown in **Fig. 3**. Corrections of these values are shown in **Fig. 4**.

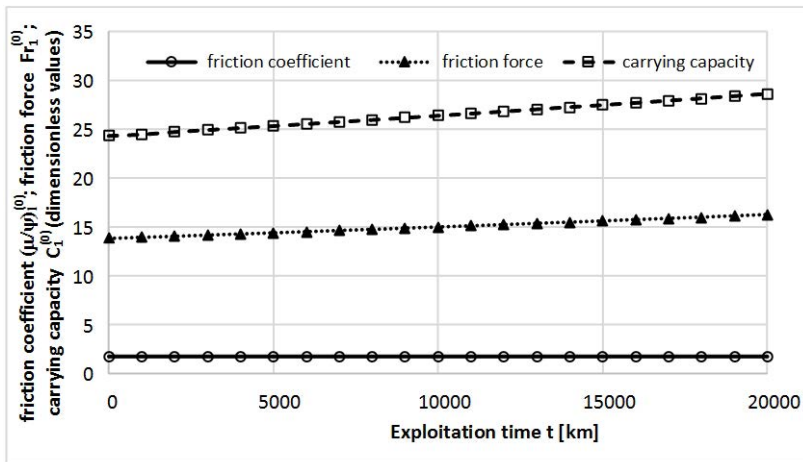


**Fig. 3. Dimensionless values: carrying capacity  $C_1^{(0)}$ , friction force  $F_{r1}^{(0)}$  and friction coefficient  $(\frac{\mu}{\psi})_1^{(0)}$  for the different exploitation intervals**

Rys. 3. Bezwymiarowe wartości: siły nośnej  $C_1^{(0)}$ , siły tarcia  $F_{r1}^{(0)}$  i współczynnika tarcia  $(\frac{\mu}{\psi})_1^{(0)}$  dla różnych czasów eksploatacji oleju

Increases of the dimensionless carrying capacity and dimensionless friction resulted from the increase of dynamic viscosity in exploitation time of the exploited oil are shown in **Fig. 3**. Due to the same influence of the dynamic viscosity on the carrying capacity and friction, the friction coefficient, as the relation of these two values, remains unchanged. In case of the dimensionless carrying capacity corrections (**Fig. 4**), we observe a decrease in this value in exploitation time (approx. 14%). Despite that, the correction of the dimensionless friction increases (approx. 32%) in exploitation time. Because the corrections are calculated according to the equation (14), we receive a very small increase of the friction coefficient correction (0.16%). It has to be indicated that, for the basic values (**Fig. 3**), we add correction values (**Fig. 4**) multiplied by the small parameter  $Q_{BR}$ .

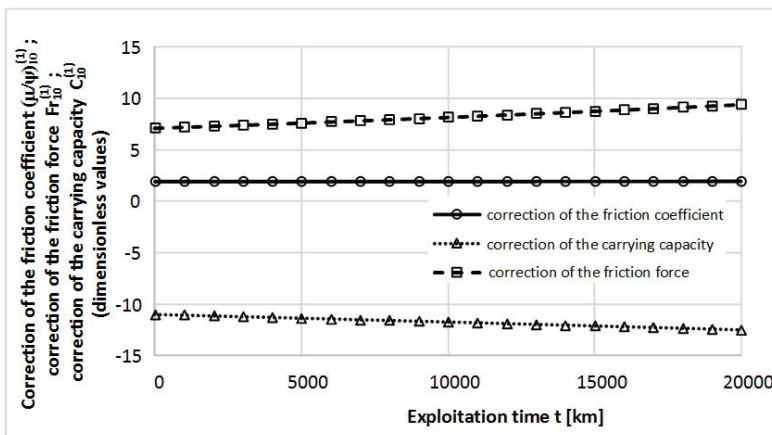


**Fig. 4. Dimensionless correction of the carrying capacity  $C_{10}^{(0)}$ , dimensionless correction of the friction  $F_{r10}^{(0)}$  and correction of the friction coefficient for the different exploitation intervals**

Rys. 4. Bezwymiarowe korekty siły nośnej  $C_{10}^{(0)}$ , bezwymiarowe korekty siły tarcia  $F_{r10}^{(0)}$  oraz korekty współczynnika tarcia  $(\mu/\psi)_{10}^{(0)}$  dla różnych czasów eksploatacji oleju

## OBSERVATIONS AND CONCLUSIONS

From the experimental research and analysis of the literature, viscosity changes can reach even 50% over time. Allowed limit states can be increased 25% or decreased by 30%, because the character of the viscosity changes in exploitation time is not linear, especially in marine engines, where: purifiers are in use.

The friction coefficient does not change while taking into account viscosity changes in exploitation time. Total dimensionless carrying capacity increases about 18% for the oil after a millage of 20000km (for  $Q_{BR} = 0.2$ ). Total dimensionless friction in this case increases to about 18%. The  $Q_{Br}$  parameter takes values from 0.2 to 0.6.

Conducted numerical analysis indicates that it is possible to take into account the influence of viscosity changes due to oil ageing on exploitation parameters of the journal bearing. Taking this fact into account at the design stage or during exploitation of the oil will allow the reduction in wear and increase the lifetime of the friction node.

## REFERENCES

1. Wang S.S., Road tests of oil condition sensor and sensing technique, Sensors and Actuators B, 2001, 73, pp. 106-111.

2. Agoston A., Ötsch C., Jakoby B., Viscosity sensors for engine oil condition monitoring – Application and interpretation of results. *Sensors and Actuators A*, 2005, 121, pp. 327–332.
3. Krupowies J., Analiza zmian parametrów użytkowych olejów smarnych okrętowych silników pomocniczych, *Zeszyty Naukowe Akademii Morskiej w Szczecinie*, 2004, Studia nr 1(73), s. 411–422.
4. Lang O.R., Steinhilper W., *Gleitlager*, Springer Verlag, Berlin-Heidelberg-New York 1978.
5. Miszczak A., Analiza hydrodynamicznego smarowania ferrocieczą poprzecznych łożysk ślizgowych, *Monografia. Fundacja Rozwoju Akademii Morskiej*, Gdynia 2006.
6. Wierzcholski K., *Mathematical Methods of Hydrodynamic Theory of Lubrication*. Politechnika Szczecińska, Monografia, nr 511, Szczecin 1993.
7. Wierzcholski K., Miszczak A., Równania hydrodynamicznej teorii smarowania cieczą o cechach modelu Rivlina Ericksena. *Zagadnienia Eksploatacji Maszyn*, 1996, Vol. 31, zeszyt 3 (106), s. 7–18.
8. Sikora G., Miszczak A.: Równania hydrodynamicznego smarowania poprzecznych łożysk ślizgowych z uwzględnieniem starzenia się oleju. *Logistyka*, 2015, 4, s. 5649–5656.
9. Galindo-Rosales F.J., Rubio-Hernández F.J., Sevilla A., Ewoldt R.H., How Dr. Malcom M. Cross may have tackled the development of An apparent viscosity function for shear thickening fluids. *Journal of Non-Newtonian Fluid Mechanics*, 2011, 166, pp. 1421–1424.
10. Kiciński J., *Hydrodynamiczne poprzeczne łożyska ślizgowe*. Wydawnictwo Instytutu Maszyn Przepływowych PAN, Gdańsk 1996.
11. Sikora G., Miszczak A., Viscosity in Exploitation Time Analysis of the Lubricating Oil Used in the Combustion Engine of the Personal Car. *Solid State Phenomena*, 2015, Vols. 220-221, pp. 271–276.

## Streszczenie

**W niniejszej pracy przedstawiono obliczenia numeryczne rozkładu ciśnienia hydrodynamicznego, siły nośnej oraz współczynnika tarcia w szczelinie poprzecznego łożyska ślizgowego smarowanego olejem silnikowym z uwzględnieniem zmian lepkości oleju od temperatury i czasu eksploatacji. W pracy nie uwzględniano zmian lepkości od ciśnienia i szybkości ścinania. Takie zmiany będą uwzględnione w innych pracach.**

**Do analizy hydrodynamicznego smarowania przyjęto laminarny przepływ cieczy smarującej oraz nieizotermiczny model smarowania łożyska ślizgowego. Jako równanie konstytutywne zastosowano klasyczny model newtonowski z uwzględnieniem zmian lepkości od temperatury i czasu eksploatacji. Do rozważań przyjęto walcowe łożysko ślizgowe o skończonej długości z gładką panewką o pełnym kącie opasania.**